

RESEARCH ARTICLE

10.1002/2015JA021307

Key Points:

- Variability of EEJ and EIA are studied over Indian and Brazilian sectors
- EIA strength show strong dependence with the IEEJ integrated up to day maximum
- A time delay is observed between the day maximum EEJ and well-developed EIA

Correspondence to:

K. Venkatesh,
venkatkau@gmail.com

Citation:

Venkatesh, K., P. R. Fagundes, D. S. V. V. D. Prasad, C. M. Denardini, A. J. de Abreu, R. de Jesus, and M. Gende (2015), Day-to-day variability of equatorial electrojet and its role on the day-to-day characteristics of the equatorial ionization anomaly over the Indian and Brazilian sectors, *J. Geophys. Res. Space Physics*, 120, doi:10.1002/2015JA021307.

Received 6 APR 2015

Accepted 25 SEP 2015

Accepted article online 30 SEP 2015

Day-to-day variability of equatorial electrojet and its role on the day-to-day characteristics of the equatorial ionization anomaly over the Indian and Brazilian sectors

K. Venkatesh¹, P. R. Fagundes¹, D. S. V. V. D. Prasad², C. M. Denardini³, A. J. de Abreu⁴, R. de Jesus^{1,3}, and M. Gende⁵

¹IP&D, Universidade do Vale do Paraíba, Sao Jose dos Campos, Brazil, ²Department of Physics, Andhra University, Visakhapatnam, India, ³Instituto Nacional de Pesquisas Espaciais, S. J. Campos, Brazil, ⁴Instituto Tecnológico de Aeronáutica (ITA), Divisão de Ciências Fundamentais, São José dos Campos - SP, Brazil, ⁵Facultad de Ciencias Astronómicas y Geofísicas, Universidad Nacional de La Plata, La Plata, Argentina

Abstract The equatorial electrojet (EEJ) is a narrow band of current flowing eastward at the ionospheric *E* region altitudes along the dayside dip equator. Mutually perpendicular electric and magnetic fields over the equator results in the formation of equatorial ionization anomaly (EIA), which in turn generates large electron density variabilities. Simultaneous study on the characteristics of EEJ and EIA is necessary to understand the role of EEJ on the EIA variabilities. This is helpful for the improved estimation of total electron content (TEC) and range delays required for satellite-based communication and navigation applications. Present study reports simultaneous variations of EEJ and GPS-TEC over Indian and Brazilian sectors to understand the role of EEJ on the day-to-day characteristics of the EIA. Magnetometer measurements during the low solar activity year 2004 are used to derive the EEJ values over the two different sectors. The characteristics of EIA are studied using two different chains of GPS receivers along the common meridian of 77°E (India) and 45°W (Brazil). The diurnal, seasonal, and day-to-day variations of EEJ and TEC are described simultaneously. Variations of EIA during different seasons are presented along with the variations of the EEJ in the two hemispheres. The role of EEJ variations on the characteristic features of the EIA such as the strength and temporal extent of the EIA crest has also been reported. Further, the time delay between the occurrences of the day maximum EEJ and the well-developed EIA is studied and corresponding results are presented in this paper.

1. Introduction

The worldwide solar-driven wind flowing across the field lines results in the *E* region *Sq*-current system that produces an intensified eastward electric field in the dayside ionosphere. At the geomagnetic equator, the *Sq* current systems of the southern and northern hemispheres merge with each other and intensify to form a jet-like current in the *E* region of the ionosphere, which is called as “equatorial electrojet.” Chapman [1951] introduced the name equatorial electrojet designating a belt approximately 600 km wide centered on the dip equator due to an electric current in the *E* region of the ionosphere around 100 km altitudes. The equatorial electrojet (EEJ) phenomena primarily caused by the strongly enhanced (Cowling) conductivity in combination with the large-scale polarization electric field and the ionospheric *E*-layer tidal winds. During some times, in the EEJ region, the horizontal component of the Earth’s magnetic field (*H*) decreases rapidly for a period of few hours, suggesting a reversal of the current direction. Based on the magnetic field observations in the African sector, Gouin and Mayaud [1967] suggested a plausible explanation for this event and named it as the “counter electrojet (CEJ).” The counter electrojet is predominant during early morning and early afternoon hours [Mayaud, 1977].

Over the geomagnetic equator, the electric and magnetic fields are mutually perpendicular to each other leading to the fountain effect, under which, the plasma is lifted to the higher altitudes. The plasma at higher altitudes diffuses along the magnetic field lines under the gravitational and pressure gradient forces resulting in the formation of a double-humped latitudinal distribution of ionization known as the equatorial ionization anomaly (EIA). The two humps of ionization on either sides of the equator around $\pm 20^\circ$ are called as the crests of the EIA, and the depleted ionization region over the equator is called as the trough of the EIA. In the presence of the well-developed EIA, the electron density over the equatorial and low latitudes exhibits significant variability with local time, latitude, and altitude. As it is described, the driving force behind the fountain

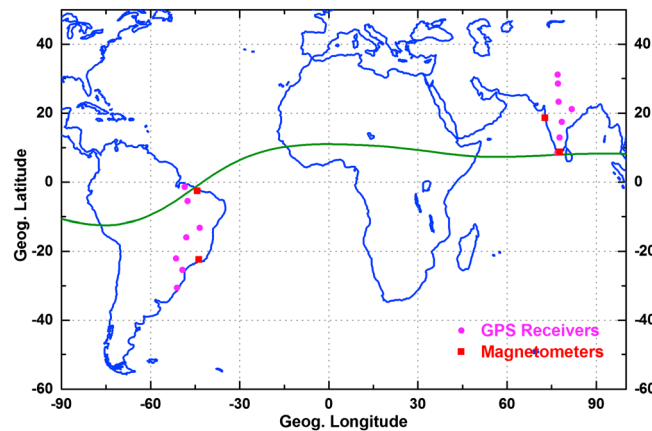


Figure 1. Map showing the locations of the GPS receivers (magenta circles) and magnetometers (red squares) over Indian and Brazilian sectors. The geomagnetic equator is shown as green colored curve.

1977; Forbes, 1981; Reddy, 1981, 1989; Stening, 1985; Rastogi, 1989; Mazaudier et al., 1993; Doumouya et al., 1998; Mazaudier et al., 2005]. During the past few decades, theoretical and scientific models of the ionospheric dynamo have been developed to explain the mechanism of the EEJ flow and its morphology [Sugiura and Cain, 1966; Sugiura and Poros, 1969; Richmond, 1973; Kane and Trivedi, 1982; Stening, 1985; Reddy, 1989; Chandra et al., 2000; Rabiou et al., 2007; Denardini et al., 2009; Abbas et al., 2012; Rastogi et al., 2013; Guizzelli et al., 2013]. Electrojet characteristics have also been simulated by assuming simple current configurations such as line current [Forbush and Casaverde, 1961], thin-band current [Chapman, 1951] and fourth degree current distribution [Fambitakoye, 1976], and thick current distribution [Onwumechili, 1967]. All these investigations revealed that the EEJ exhibits significant diurnal, seasonal, day-to-day, and longitudinal variabilities. Therefore, a simultaneous study of the day-to-day characteristics of EEJ and EIA is useful in understanding the quantitative role of EEJ on the equatorial and low-latitude ionospheric electron density variabilities. This will be helpful in achieving improved accuracy in the estimation of equatorial and low-latitude ionospheric total electron content (TEC) and corresponding range delays required for the satellite based communication and navigation applications.

The geomagnetic equator passes through the Indian and Brazilian sectors, while India is on the northern hemisphere and Brazil is on the southern hemisphere. Simultaneous observations using magnetometers and GPS-TEC receivers at multiple locations over the Indian sector in northern hemisphere and Brazilian sector in southern hemisphere are used to understand the day-to-day variability of EEJ and its role on the characteristics of the EIA and electron density distribution, the results of which are discussed in this paper.

2. Data and Analysis

The horizontal components of the Earth's magnetic field measured over an equatorial station Tirunelveli and an off-equatorial station Alibag in the Indian sector and from an equatorial station Sao Luiz and an off equatorial station Vassouras in the Brazilian sector during the low solar activity year 2004 (mean $R_z = 41$) are used. The magnetometer measurements from the Indian sector are obtained from the Indian Institute of Geomagnetism online data portal (<http://wdciig.res.in/WebUI/Home.aspx>). In the Brazilian sector, the magnetometers are from the Embrace Network [Denardini et al., 2013]. The locations of these magnetometers are shown as red colored filled squares in Figure 1, and corresponding coordinates are given in Table 1. The H -component values of the Earth magnetic field at the above four locations are normalized to the difference between the H -component values and the mean midnight values for the five quietest days. Quiet days are considered as provided by the World Data Center for Geomagnetism, Kyoto (<http://wdc.kugi.kyoto-u.ac.jp/qddays/index.html>). Finally, variations of the EEJ ground strength are estimated by calculating the difference between the ΔH values at equatorial and off equatorial stations over Indian and Brazilian sectors.

effect is the $E \times B$ drifts over the equator being controlled by the strength of the EEJ. Thus, the EEJ and EIA are the most typical equatorial and low-latitude ionospheric phenomena, and the characteristics of EEJ play a vital role on the electron density distribution over equatorial and low latitudes.

Since the discovery of the EEJ at Huancayo (Peru) near the dip-equator, several studies have been carried out to explain the generating mechanism of the equatorial electrojet (EEJ) [Baker and Martyn, 1953; Chapman and Bartels, 1940]. Reviews on EEJ and CEJ have been made by different researchers [Richmond, 1973; Kane, 1976; Mayaud,

Table 1. Coordinates of the GPS Receivers and Magnetometers Over Indian and Brazilian Sectors Used in the Present Study

Station Name	Code	Geog. Lat.	Geog. Long.	Dip Lat.
<i>GPS Receivers in the Indian Sector</i>				
Trivandrum	TRIV	8.47°N	76.91°E	0.4°N
Bangalore	BNGL	12.9°N	77.68°E	6.0°N
Hyderabad	HYDE	17.4°N	78.47°E	11.4°N
Raipur	RAIP	21.2°N	81.74°E	15.8°N
Bhopal	BHOP	23.3°N	77.34°E	18.6°N
Delhi	DELH	28.6°N	77.21°E	25.1°N
Shimla	SHIM	31.1°N	77.07°E	28.2°N
<i>GPS Receivers in the Brazilian Sector</i>				
Belem	BELE	1.4°S	48.45°W	2.8°N
Empress	IMPZ	5.5°S	47.48°W	0.8°S
Bom Jes. da Lapa	BOMJ	13.3°S	43.41°W	7.6°S
Brazilia	BRAZ	15.9°S	47.9°W	9.8°S
Pres. Prudente	UEPP	22.1°S	51.4°W	14.9°S
Curitiba	PARA	25.4°S	49.21°W	17.4°S
Porto Alegre	POAL	30.6°S	51.11°W	21.2°S
<i>Magnetometers in the Indian Sector</i>				
Tirunelveli	TNVL	8.7°N	77.8°E	0.4°N
Alibag	ALBG	18.6°N	72.8°E	13.1°N
<i>Magnetometers in the Brazilian Sector</i>				
Sao Luiz	SALU	2.58°S	44.2°W	0.6°S
Vassouras	VSSR	22.4°S	43.6°W	15.3°S

Two different chains of GPS-TEC receivers along the common meridians of 77°E in the Indian (northern hemisphere) sector and 45°W in the Brazilian (southern hemisphere) sector during 2004 are used to study the characteristics of the EIA. These two chains of GPS receivers cover from equator to the anomaly crest and beyond. The locations of these receivers are shown in Figure 1 and corresponding coordinates are provided in Table 1. The GPS receivers over the Indian sector are from a network installed jointly by the Indian Space Research Organization and the Airport Authority of India under the Indian GPS Aided GEO Augmented Navigation program for making the continuous measurements of TEC and scintillation index. The TEC data over the Brazilian sector are obtained from the database of the Instituto Brasileiro de Geografia e Estatística (IBGE) network of GPS receivers except for the station Brasilia (BRAZ), which is downloaded from the Goddard Space Flight Center (GSFC) NASA website (<ftp://cddis.gsfc.nasa.gov/pub/gps/data/daily/>). The differential delay technique is used to compute the TEC values from the dual frequency measurements at L_1 (1575.42 MHz) and L_2 (1227.60 MHz) frequencies.

Thus, derived TEC and EEJ values during the year 2004 are simultaneously studied to explain the variability of EEJ and EIA in the equatorial and low latitudes over Indian and Brazilian sectors. To study the seasonal characteristics of EEJ and TEC, the data are grouped into three Lloyd's seasons, namely, equinox (March, April, September, and October), winter (northern winter: January, February, November, and December; southern winter: May, June, July, and August), and summer (northern summer: May, June, July, and August; southern summer: January, February, November, and December), and the corresponding results are discussed.

3. Results and Discussion

3.1. Diurnal, Seasonal, and Day-To-Day Variability of EEJ and TEC

The diurnal variations of TEC over seven different locations along the common meridian of 77°E in the Indian sector are presented as mass plots in Figure 2 along with the diurnal variations of EEJ during three different seasons. Three vertical columns refer to seasons, namely, equinox, northern winter, and northern summer, respectively. The EEJ variations are presented in the first row, and the TEC variations at different stations are presented in the remaining rows. The seasonal mean diurnal values are plotted as thick lines with blue color for EEJ and with red color for TEC. It is seen from this figure that the equatorial electrojet is stronger during day time from 08:00 to 16:00 LT with maximum values during equinoctial months. Significant day-to-day variability in the diurnal variation of EEJ can be seen from these mass plots. Counter electrojet

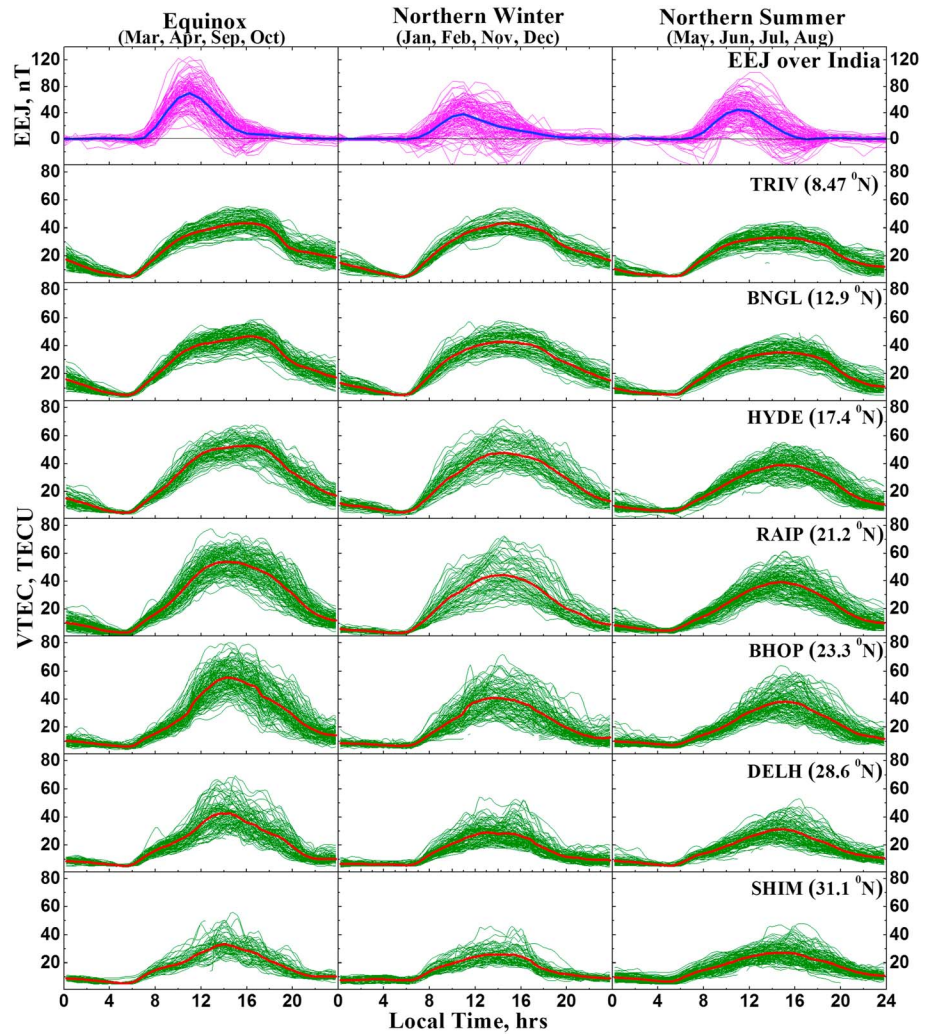


Figure 2. Mass plots showing the diurnal variations of EEJ (first row) and TEC over seven different locations from equator to the anomaly crest and beyond in the Indian sector during three different seasons, namely, equinox, northern winter, and northern summer of the year 2004.

(CEJ) events are found to be more frequent during winter and summer months. From the seasonal mean diurnal variations, the maximum EEJ is found to be around 60 nT during equinox and around 40 nT during winter and summer months.

The diurnal variations of TEC presented for seven different stations from equator to the anomaly crest and beyond also show higher values during equinoctial months compared to winter and summer months. The day maximum values of TEC increase from equator (TRIV) to the anomaly crest (RAIP and BHOP) and decrease beyond during the three seasons. Significant day-to-day variability in TEC is observed at all the locations, and greater variability is found around the anomaly crest locations. It can be inferred from these plots that the seasonal and day-to-day characteristics in the variations of EEJ and TEC are similar.

Figure 3 shows the diurnal variations of EEJ and TEC as mass plots along with the seasonal mean values during equinox, southern winter, and southern summer over the Brazilian sector. Three panels in the first row represent the diurnal variations of EEJ, while the other panels in remaining rows represent the diurnal variation of TEC at different locations during three seasons. It is observed from these figures that the TEC at different locations show higher values during equinoctial months and lower values during winter months. The day maximum values of TEC are found to be higher at and around the anomaly crest locations. The day-to-day variability in the diurnal variation of TEC is observed at all the locations during the three seasons, and this variability is higher around the anomaly crest locations during equinoctial months. The seasonal

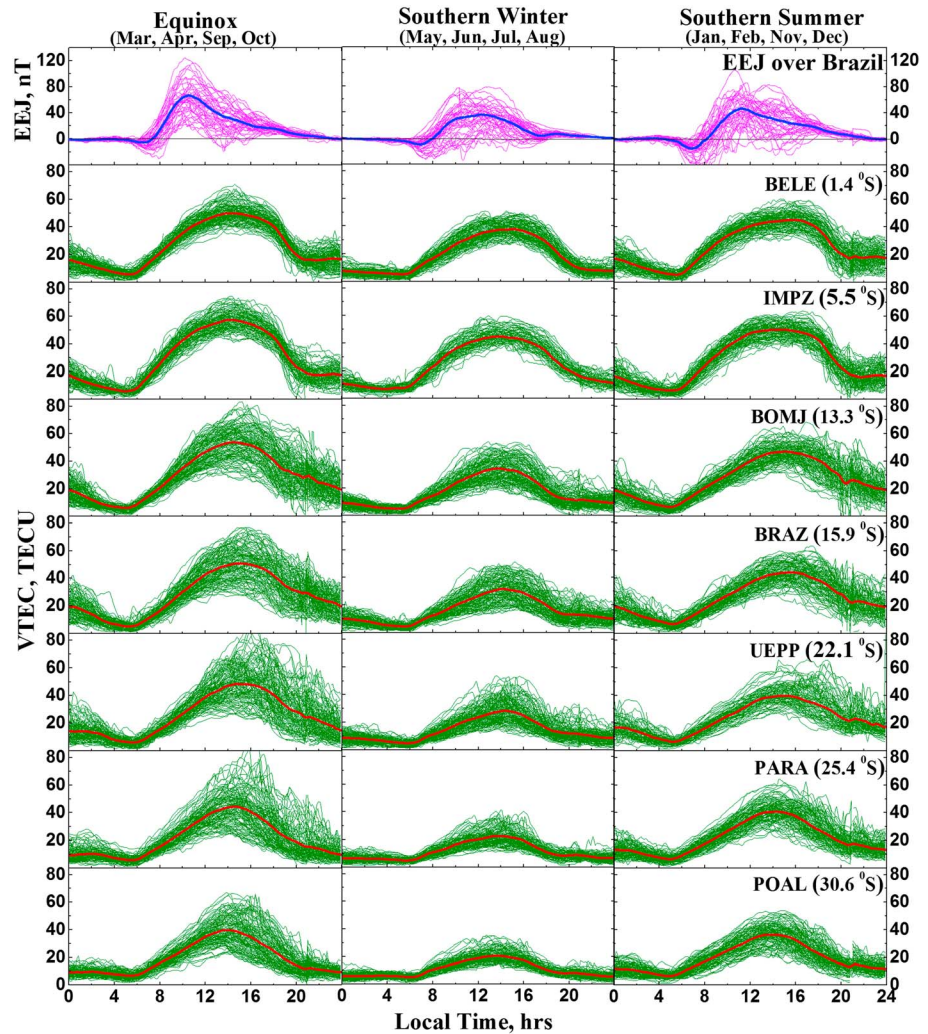


Figure 3. Mass plots showing the diurnal variations of EEJ (first row) and TEC over seven different locations from equator to the anomaly crest and beyond in the Brazilian sector during three different seasons, namely, equinox, southern winter, and southern summer of the year 2004.

and day-to-day variabilities in TEC variations over the equatorial and low-latitude sectors have been reported in the earlier studies using measurements from different parts of the globe [Abdu et al., 1996; Mannucci et al., 1998; Brunini et al., 2003; Jee et al., 2005, Bagiya et al., 2009; Venkatesh et al., 2014; Shimeis et al., 2014, 2015, and references therein].

It is seen from Figure 3 that the EEJ over Brazil shows higher values during equinoctial months and lower values during southern summer months. During equinoctial and summer seasons, after attaining the day maximum, the EEJ slowly decays and reaches the minimum level around the late-night hours. Whereas in the Indian sector (Figure 2), the EEJ reaches to the minimum level by the evening hours. A detailed insight in to diurnal variations of EEJ revealed that in the Indian sector, the EEJ reaches the day minimum level between 1600 and 1800 h LT during more than 60% of the days. Whereas in the Brazilian sector, the EEJ reaches the day minimum after 2000 h LT during more than 70% of the days. From the diurnal variations of EEJ reported by Doumouya et al. [1998] over African sector, it is seen that the EEJ reaches the day minimum in later hours during equinoctial months compared to that during other seasons. Mazaudier et al. [2006] studied the longitudinal differences in the Earth magnetic field variations between Indian and Vietnamese sectors and reported that the magnetic field is stronger in the Vietnamese longitudes than in the Indian longitudes. Chandrasekhar et al. [2014] have also reported significant longitudinal variations in the EEJ characteristics using the magnetometer measurements in the Indian sector. It has also been shown that

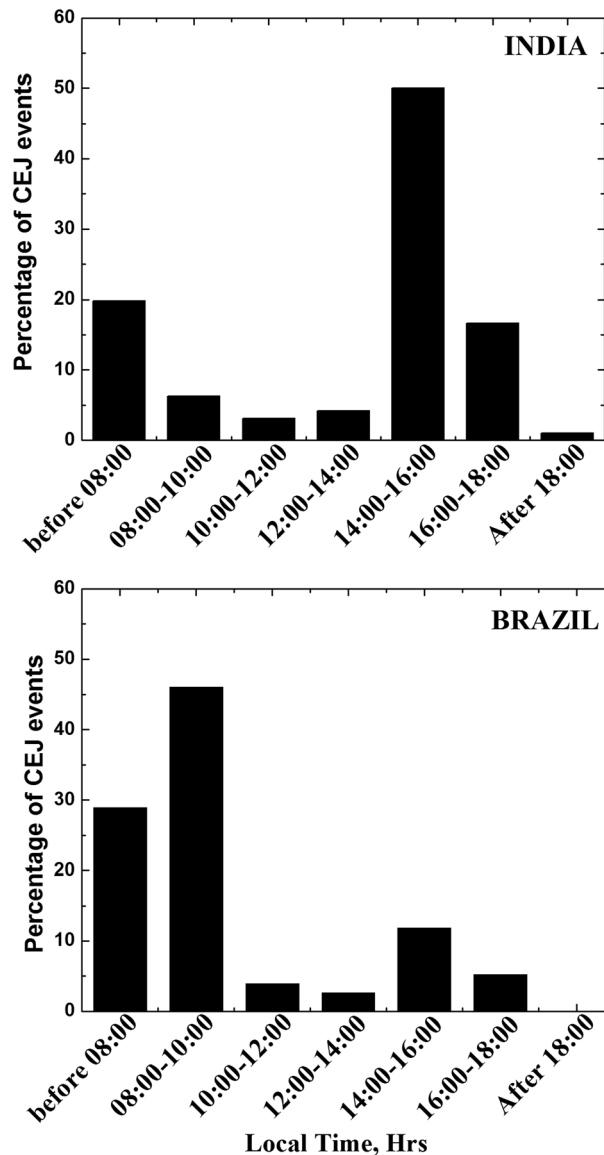


Figure 4. Histograms showing the variation of the percentage of CEJ events at different local times in the Indian and Brazilian sectors during the year 2004.

the EEJ is strongest in South America and weakest in Indian sector with a secondary minimum in the Atlantic sector and secondary maximum in the western African sector [Doumouya et al., 2003; Doumouya and Cohen, 2004].

The diurnal variations of EEJ over Brazil also show that the CEJ events are more frequent during winter and summer months compared to those during equinoctial months. Mayaud [1977], Doumouya et al. [1998], and Denardini et al. [2009] have also reported that the CEJ events are more frequent and clear during solstice months over African and Brazilian sectors. Further, it is also observed that the CEJ events are more frequent during presunrise hours compared to those during the evening hours. Simultaneous comparison of the diurnal variations of EEJ over Indian and Brazilian sectors revealed that these morning CEJ events are more frequent in the Brazilian sector compared to the Indian sector.

To study the local time variations in the occurrence of CEJ, the percentage of CEJ events at different local times is presented as histograms in Figure 4 for Indian and Brazilian sectors. It can be seen from this figure that 65% of the total CEJ events in the Indian sector are during afternoon, while 50% of the events are observed between 1400 and 1600 h LT. In the Brazilian sector, nearly 75% of the total CEJ events are observed in the morning before 1000 h LT. From the seasonal behavior of CEJ events described in Figure 2, it may be noted here that among the 50% CEJ

events in the afternoon hours over Indian sector, most of the cases occur during winter and summer months. Further, in the Brazilian sector, the major contribution to the 75% of morning CEJ events occurs during winter and summer months as it is evidenced in Figure 3. Using the EEJ measurements in the African sector, Doumouya et al. [1998] reported that roughly 50% of the CEJ events are observed during morning hours. Fambitakoye and Mayaud [1976] have also reported CEJ events between 7 and 8 h LT during the central African experiment. Muniz [1992] reported that the CEJ events do not occur at the same local time in different longitudes since there is a modulation effect in CEJ events due to Moon. Alex and Mukherjee [2001] also compared the CEJ events at two equatorial stations Trivandrum and Addis Ababa and reported that there are differences in CEJ events when observed in different longitudinal sectors.

Further, significant day-to-day variability is observed in the diurnal variations of EEJ over Indian and Brazilian sectors during the three different seasons. Day-to-day variability in EEJ has also been reported using the measurements in the African sector by Abbas et al. [2012] and in the Indian sector by Chandrasekhar et al. [2014]. This EEJ variability can be attributed to the variability of the ionospheric processes and physical structure

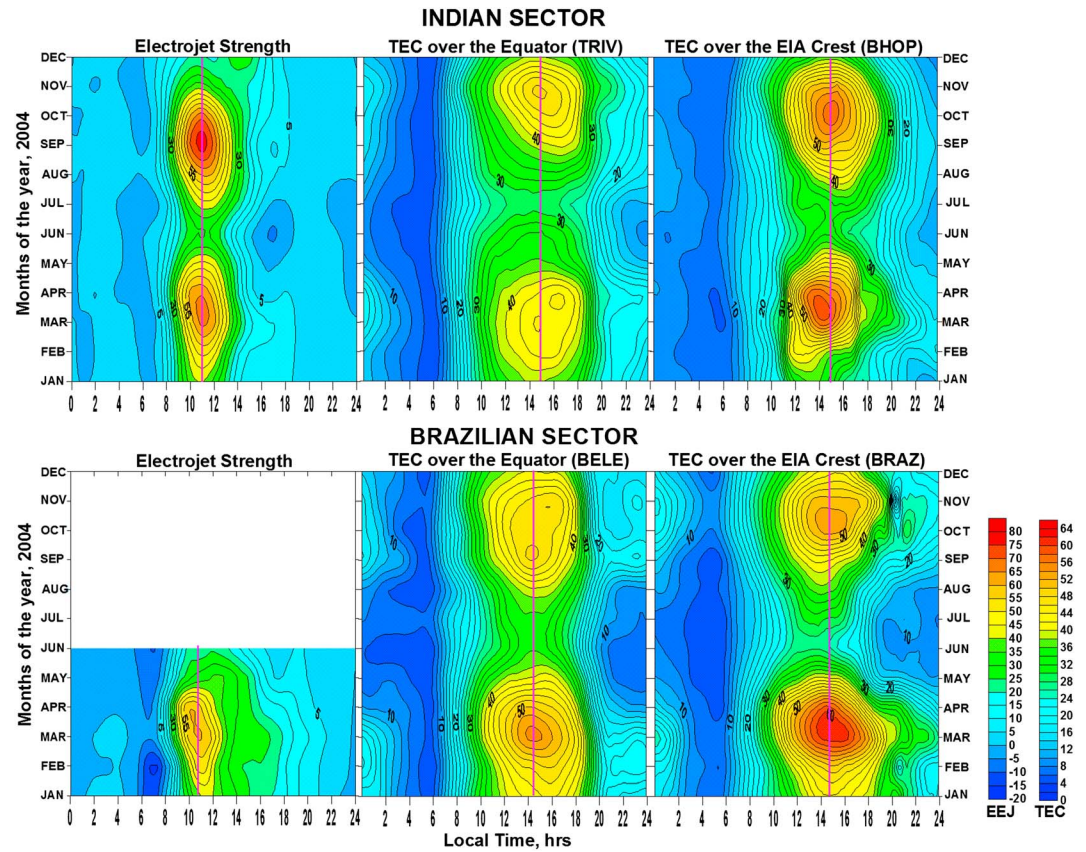


Figure 5. Contour plots showing the diurnal variation of EEJ and TEC over the equator and anomaly crest locations in the Indian and Brazilian sectors during the year 2004.

such as conductivity and wind structure [Abbas *et al.*, 2012]. Yamazaki *et al.* [2014] reported that the irregular variability of the neutral wind produces day-to-day variations in the daily range of $Sq(H)$ near the magnetic equator causing the electrojet variability from day-to-day. They have also shown that the zonal polarization electric field of the zonal wind is the main source of the day-to-day variations of equatorial electrojet. In the present study, simultaneous observations of the diurnal, seasonal, and day-to-day characteristics of EEJ and TEC in the Indian and Brazilian sectors reveal that both the parameters show equinoctial maxima with significant day-to-day variability in the day maximum values. Particularly, in both the sectors, the variabilities in TEC around the anomaly crest locations are in coincidence with the EEJ variabilities during three different seasons.

3.2. Semi Annual Variations in EEJ and TEC

The EEJ values over Indian and Brazilian sectors along with the TEC over two equatorial stations (TRIV in India and BELE in Brazil) and two anomaly crest locations (BHOP in India and BRAZ in Brazil) are analyzed to study the semiannual characteristics. Monthly mean diurnal variations of EEJ and TEC during the year 2004 are presented as contour plots in Figure 5. Figure 5 (top) shows the variations of EEJ and TEC over Indian sector, while Figure 5 (bottom) represents those over the Brazilian sector. It is readily seen from these contours that both EEJ and TEC have shown semiannual variations with two peaks during equinoctial months of March/April and September/October. Chandrasekhar *et al.* [2014] have studied the EEJ variations over the Indian sector and reported the semiannual behavior with two peaks in the equinoctial months. Magnetic field observations from other regions of the globe have also revealed the semiannual behavior in the EEJ variations [Doumouya *et al.*, 1998; Mazaudier *et al.*, 2005, 2006; Abbas *et al.*, 2012]. It is seen from this figure that the TEC values over the equatorial stations are lower compared to those over the anomaly crest locations. However, the semiannual behavior in TEC over equator and anomaly crests are similar to that observed in the variations of EEJ. Over the contours of EEJ and TEC, magenta colored vertical lines are drawn along the

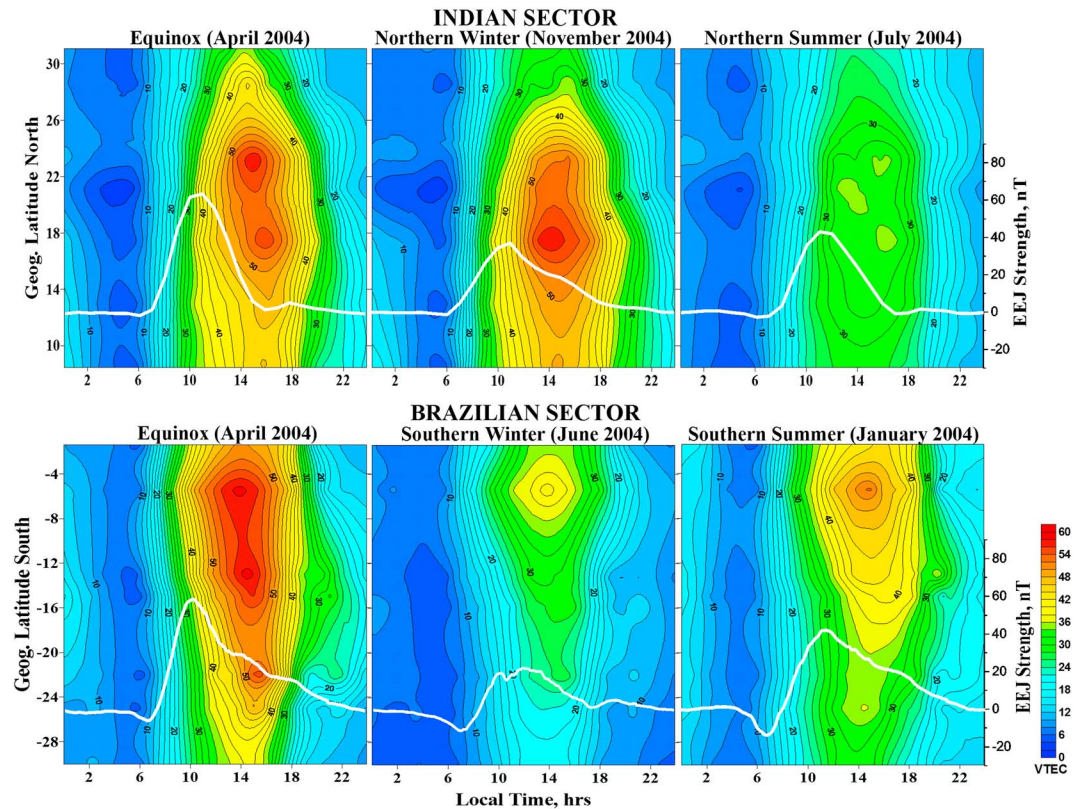


Figure 6. Equatorial ionization anomaly variations during three different months representing three seasons equinox, winter, and summer in the Indian and Brazilian sectors. The simultaneous monthly mean diurnal variations of EEJ values are plotted on the corresponding contours.

day maximum covering the two semiannual peaks. It can be noticed from these magenta lines that the maximum in the diurnal variation of EEJ is observed around 1100 h LT, while the day maximum is seen around 1500 h LT in the diurnal variation of TEC in both the hemispheres. This indicates that after the occurrence of the day maximum in EEJ, there exists a time lag to reach the day maximum level in TEC.

3.3. Role of EEJ Variations on the Formation and Characteristics of the EIA Crest

The characteristic features of the EIA such as the strength, location, and the extent of the anomaly are the parameters required to understand the electron density variability in the equatorial and low-latitude sectors. The TEC data from two different chains of stations over Indian and Brazilian sectors are analyzed to derive the characteristic features of the EIA. The simultaneous values of the EEJ strength are used to study its role on the formation and development of the EIA crest, and the corresponding results are presented in the following sections.

3.3.1. Variations of EIA and EEJ During Different Seasons

Figure 6 represents the contour plots of TEC showing the equatorial ionization anomaly during different months representing equinox, winter, and summer seasons over Indian and Brazilian sectors. The corresponding monthly mean diurnal variations of EEJ are superimposed as white colored curves on the EIA contours. The three contours on the top row show the EIA variations over Indian sector, while the three contours in the bottom row represent those of the Brazilian sector. It is observed that the EIA crest is strong during equinoctial months over the two hemispheres. The anomaly crest is found to be weak during summer (July 2004) in the northern hemisphere and during winter (June 2004) in the southern hemisphere. Also, the location of the EIA crest is found to be farther from the equator during equinoctial months compared to that during winter and summer months in both hemispheres. Simultaneously, the white colored monthly mean EEJ shows strong peak during equinoctial months with the day maximum of about 60 nT in both the sectors, which is in coincidence with the observed strong EIA. Further, during northern summer (July 2004) and southern winter (June 2004), the EEJ is found to be weak showing the day maximum of about 40 nT in the Indian sector and about 20 nT in the Brazilian sector, which is also in coincidence with the weak EIA seen in the TEC variations. These observations indicate that the

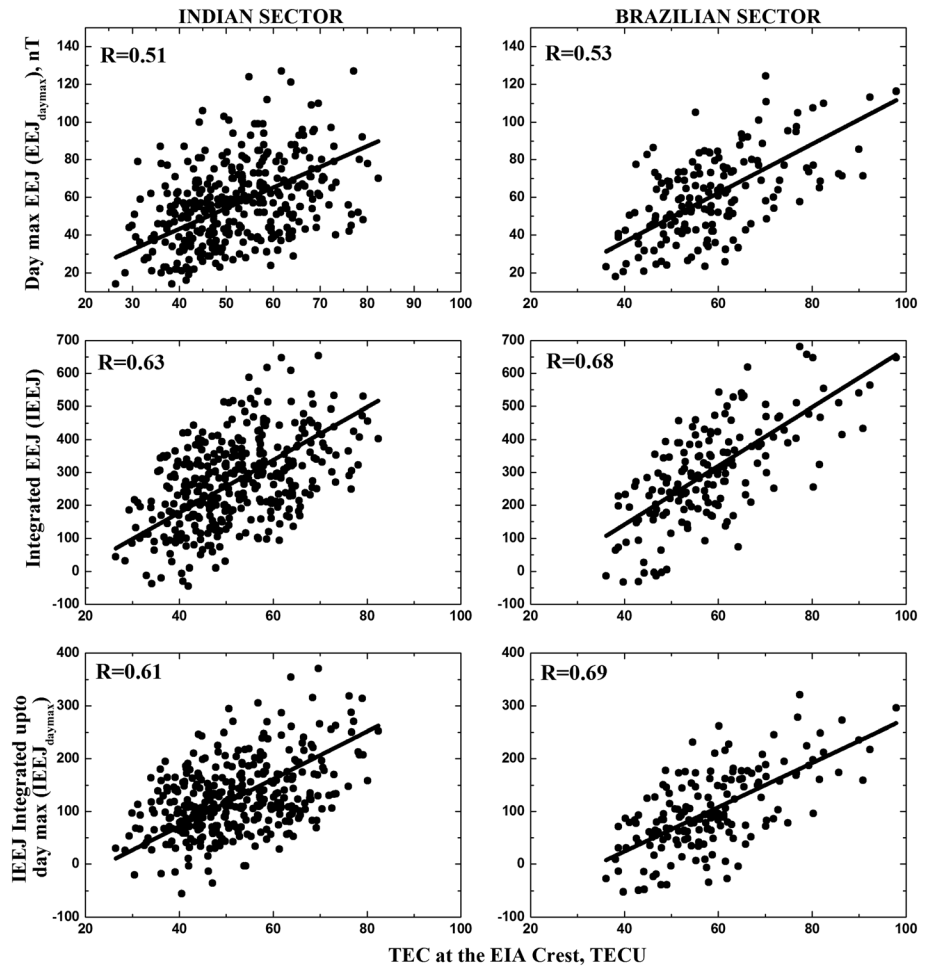


Figure 7. Scatterplot showing the variations of the TEC at the EIA crest with day maximum EEJ, integrated EEJ, and integrated EEJ up to day maximum during the year 2004 over Indian and Brazilian sectors.

strength of the EIA is well dependent on the corresponding EEJ variations. The following section describes the dependence of the EIA crest on different EEJ parameters.

3.3.2. Strength of the EIA Crest: Dependence With Different EEJ Parameters

As it is described, in the presence of the eastward electric field, the fountain effect leads to the formation of two crests on either sides of the equator. As the strength of the electric field increases, more plasma is lifted to higher altitudes over the equator and it will be transported to farther latitudes from equator. To understand the dependency of strength of the EIA crest on the diurnal characteristics of EEJ, three different parameters are computed from EEJ diurnal variations. The first one is the day maximum value of EEJ, which is termed as EEJ_{daymax} . The second parameter is the integrated EEJ (IEEJ), calculated by integrating the EEJ during the complete day which indicates the EEJ strength for the whole day. Further, as an indicative parameter of the strength of EEJ up to the day maximum, the EEJ is integrated up to the day maximum level and termed as $IEEJ_{daymax}$, which is considered as the third parameter.

Scatterplots between the EIA strength (TEC at the EIA crest) and the aforementioned three EEJ parameters (EEJ_{daymax} , IEEJ, and $IEEJ_{daymax}$) have been plotted for Indian and Brazilian sectors and presented in Figure 7. The three panels in left column show the variations of TEC at EIA crest with three EEJ parameters over Indian sector, while the other three panels in the right column represent those over the Brazilian sector. All these plots indicate that there exists a positive dependence of the EIA strength on three different EEJ parameters. It is seen that the scatter between EIA strength and EEJ_{daymax} is greater compared to those between EIA strength and integrated EEJ values at the two different sectors. The correlation coefficient values between EIA strength and EEJ_{daymax} are also found to be lower compared to those with IEEJ and $IEEJ_{daymax}$ over the two sectors.

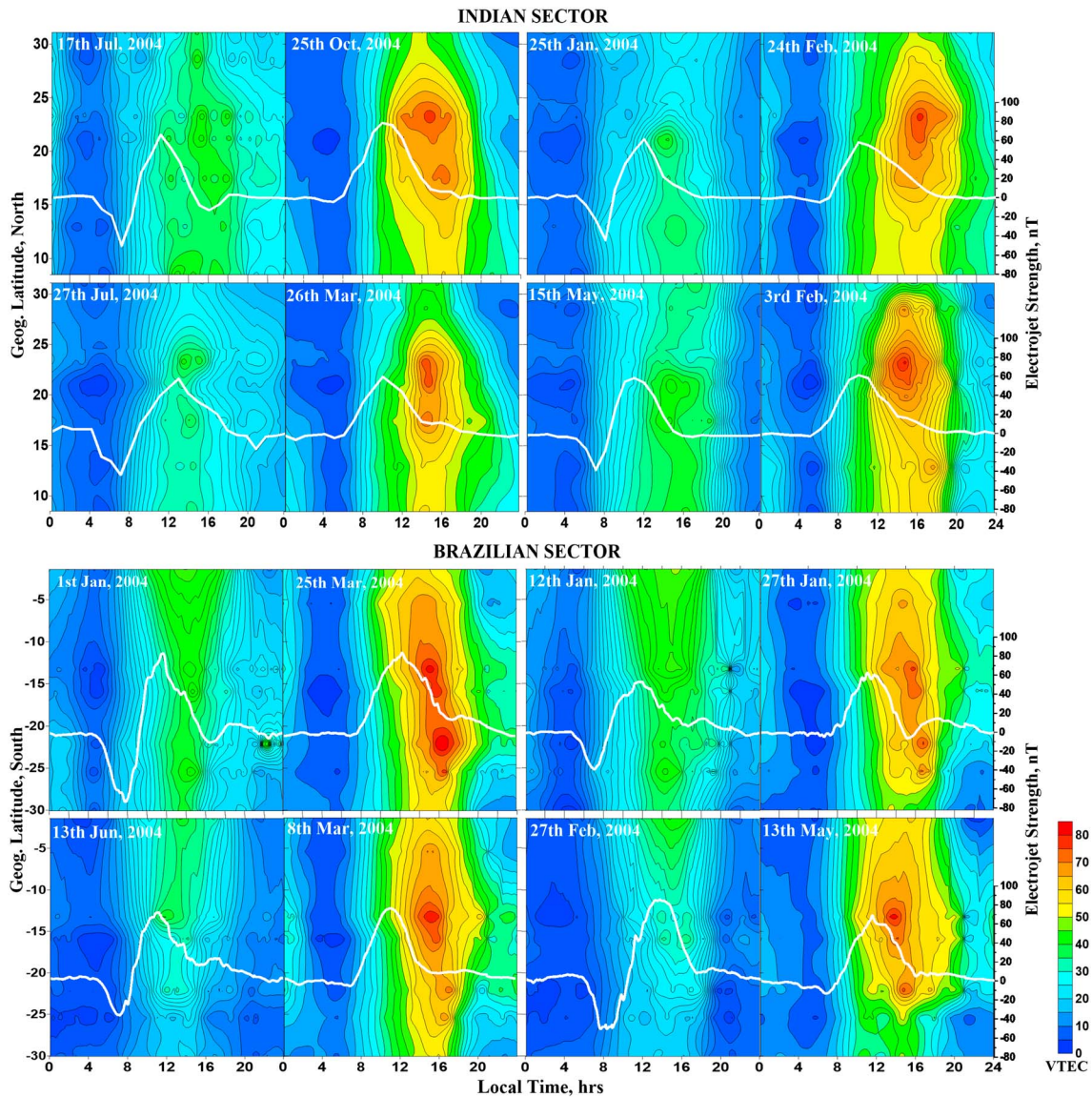


Figure 8. Examples showing the equatorial ionization anomaly variations along with the corresponding diurnal variations of EEJ over Indian and Brazilian sectors.

This indicates that the strength of the EIA is more dependent on integrated EEJ values (IEEJ and $IEEJ_{daymax}$) compared to that of the day maximum EEJ. Further, the two different cases with the IEEJ and $IEEJ_{daymax}$ have shown similar correlation coefficient values in both the sectors. This observation indicates that for the formation of the EIA crest, the role of the strength of EEJ up to the day maximum ($IEEJ_{daymax}$) is more significant compared to the influence of EEJ after the day maximum.

To understand the role of the $IEEJ_{daymax}$ on the strength of the EIA crest, various examples of the EIA along with the corresponding EEJ diurnal variations over Indian and Brazilian sectors have been plotted and presented in Figure 8. The eight contours in the top two rows represent the examples over the Indian sector, while the remaining eight contours in the bottom two rows represent the examples over the Brazilian sector. It is seen from the example on 17 July 2004 in the Indian sector that there is a strong counter electrojet in the morning hours, and later, the EEJ reaches to a day maximum of about 70 nT. In this case, the anomaly is not clearly observed and the EIA crest is not formed. In the adjacent contour on 25 October 2004, there is no counter electrojet and the day maximum EEJ is around 70 nT. A well-developed equatorial anomaly is seen on this day with a strong EIA crest. In these four different sets of examples, even though the day maximum values of EEJ are nearly similar and occurred around the same local time, the anomaly can be seen on the days

without morning CEJ and it is absent during the days with morning CEJ. During the four CEJ days (17 July 2004, 25 January 2004, 27 July 2004, and 15 May 2004) there is counter electrojet in the morning hours and the $IEEJ_{daymax}$ is less and is not producing sufficient uplift for the plasma over the equator for the formation of EIA crest. During the other four cases (25 October 2004, 24 February 2004, 26 March 2004, and 3 February 2004) there is no morning CEJ and the $IEEJ_{daymax}$ is strong and is producing enough uplift for the plasma over the equator leading to the formation of the strong EIA crest.

Similarly, different sets of examples are presented over the Brazilian sector. In the examples on four CEJ days (1 January 2004, 12 January 2004, 13 June 2004, and 27 February 2004), a strong counter electrojet is seen in the morning hours leading to a smaller value of $IEEJ_{daymax}$ resulting in the absence of the formation of clear anomaly crest. During the other four examples without morning CEJ (25 March 2004, 27 January 2004, 8 March 2004, and 13 May 2004), $IEEJ_{daymax}$ gives strong support to the formation of the clear anomaly with a strong EIA crest. All these examples presented over Indian and Brazilian sectors clearly indicate that the EEJ strength up to the day maximum ($IEEJ_{daymax}$) plays significant role on the formation and development of the EIA crest. This is also in agreement with the observations made from scatterplots in Figure 7 using the data for the year 2004, where the $IEEJ_{daymax}$ shows nearly similar correlation compared to that of the $IEEJ$ and more correlation compared to those with EEJ_{daymax} .

3.3.3. Role of the Diurnal Variation of EEJ on the Temporal Extent of the EIA Crest

Once the well-developed equatorial anomaly is formed, it may start decaying soon or may exist for some time and then start decaying to the normal conditions. Therefore, the duration of the existence of the anomaly is another important aspect to understand the electron density variability over the equatorial and low latitudes. To study the effect of EEJ variations on the temporal extent of the EIA, different examples of the anomaly along with EEJ diurnal variations are presented in Figure 9. The six contour plots in the top two rows represent different examples over Indian sector, and the remaining six contours in the bottom two rows represent the examples over Brazilian sector. The corresponding EEJ diurnal variations are plotted as white colored curves on each of the contours. From the three contours in the first row over the Indian sector, it is seen that the electrojet show three different diurnal characteristics. On 12 October 2004, the electrojet exhibits a sharp day maximum around 1000 h LT. The anomaly on this day is strong and exists for only a short duration. In the second example on 23 October 2004, the EEJ shows a broad day maximum between 08:00 to 14:00 h LT. On this day, the strong anomaly is seen for a long duration of more than 4 h. Further, in the third example on 19 July 2004, the EEJ shows a double humped structure with two peaks around 10:00 and 14:00 h LT. Surprisingly, from the electron density distribution over the EIA crest on this day, it is seen that a weak anomaly is formed around noon hours, which decays for some time, and later, a well-developed anomaly is formed and it stays for few hours.

Similarly, over the Brazilian sector, the EEJ variations on 8 April 2004 show a sharp day maximum and the corresponding anomaly is very strong and exists for a short duration. On the other day of 2 May 2004, the EEJ shows a broad day maximum, while the anomaly is also seen for a long duration of about 4 h. In the other example on 1 February 2004, the EEJ shows double humped structure with two peaks around 11:00 and 16:00 h LT and the corresponding anomaly on this day shows two weak crests. Even though the cases of two crests are very rare, these type of examples give more evidence about the role of EEJ on the EIA characteristics. Different examples presented in Figure 9 over Indian and Brazilian sectors indicate that on each particular day, the diurnal characteristics of the EEJ play a vital role on the structure and temporal extent of the EIA crest.

3.3.4. Time Delay Between the Occurrences of the Day Maximum EEJ and the Well-Developed EIA

It is mentioned in section 3.2 from Figure 5 that there is a time lag between the occurrences of the day maximum EEJ and the day maximum TEC over Indian and Brazilian sectors. Also, different cases presented in various contours to describe the characteristics of the EIA (Figures 6, 8, and 9) and indicate that there is a time lag between the day maximum EEJ and the well-developed EIA crest. To understand the variations of this time difference in detail, the day-to-day EEJ and EIA variations over the two sectors during the year 2004 are analyzed. The time differences between the occurrences of day maximum EEJ and well-developed anomaly are calculated, and the results are presented in Figure 10 as histograms for various time difference values. Figure 10 (top) shows the percentage of cases for each half an hour over Indian sector, and Figure 10 (bottom) shows those over the Brazilian sector. It is seen from these histograms that the time difference between the occurrences of day maximum EEJ and well-developed EIA varies from a minimum of 3 h to a maximum of about 5 h over the two different sectors. Further, it is clearly seen from these histograms that

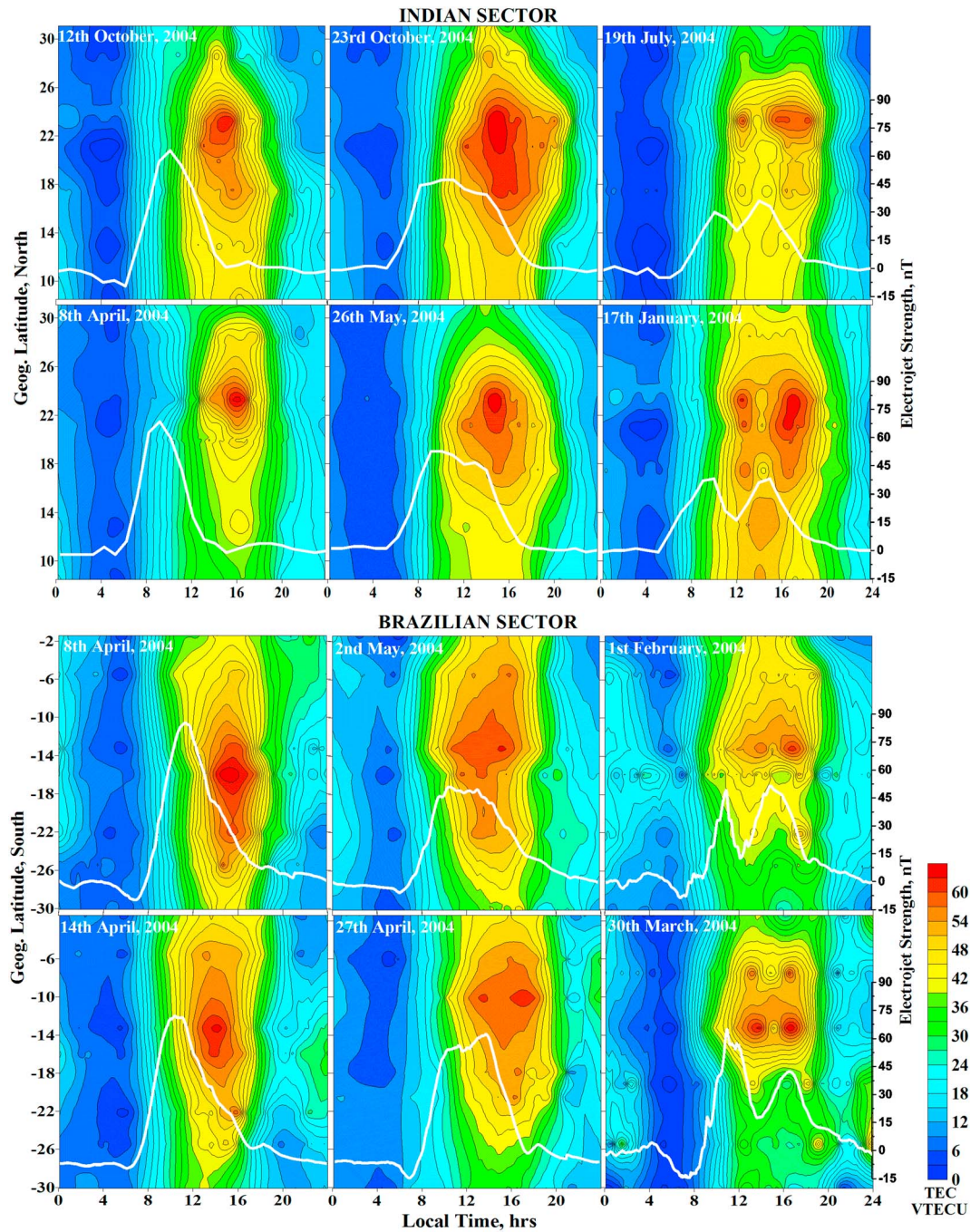


Figure 9. Contour plots showing the variations of the EIA crest with respect to the variations in the diurnal characteristics of the EEJ over Indian and Brazilian sectors.

nearly 80% of the cases have a time difference of 3:30 to 4:30 h over both Indian and Brazilian sectors. It can be inferred from these observations that it takes around 4 h to form a well-developed EIA crest after the occurrence of the day maximum in the diurnal variation of EEJ.

4. Summary

Variabilities in the equatorial electrojet and the equatorial ionization anomaly are simultaneously studied to understand the role of EEJ on the EIA characteristics in the Indian (northern hemisphere) and Brazilian

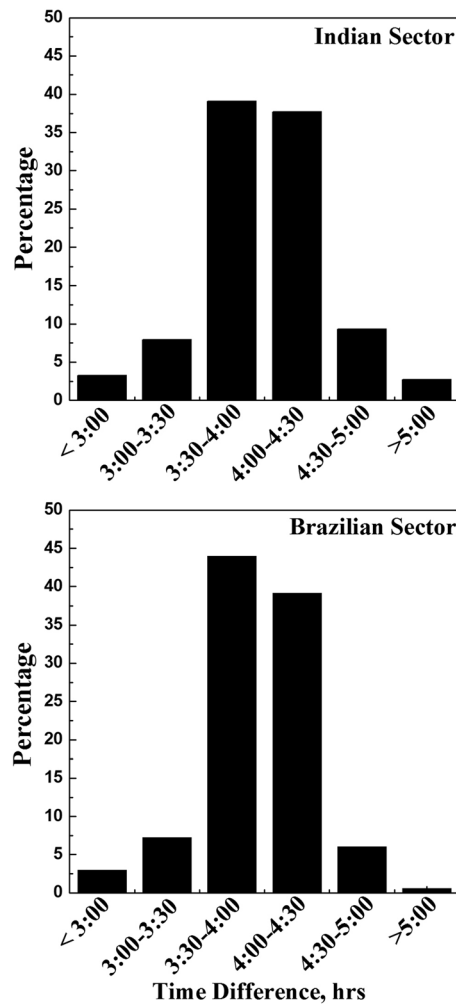


Figure 10. Histograms showing the variation of the time difference between the occurrences of day maximum EEJ and well-developed EIA crest in the Indian and Brazilian sectors during the year 2004.

The strength of the EIA during different seasons is in agreement with the strength of the EEJ over the two sectors. The strength of the EIA has shown good correlation with the integrated EEJ values ($IEEJ$ and $IEEJ_{daymax}$) compared to the day maximum EEJ. It is also found that the integrated EEJ strength up to the day maximum ($IEEJ_{daymax}$) plays a vital role on the formation of the EIA. For each particular day, the temporal extent of the well-developed EIA crest and its characteristics have shown significant dependence with the corresponding diurnal characteristics of the EEJ. Further, it is observed that after the occurrence of the day maximum in the EEJ, there exists a time delay for the formation of the well-developed EIA. In major number of cases, this delay is found to vary around 4 h. It may be inferred from the present study over the Indian and Brazilian sectors that the diurnal variations of the EEJ have significant control on the formation as well as the development of the EIA. The two important aspects observed in this analysis are (i) the dependence of the EIA strength on the $IEEJ_{daymax}$ and (ii) the time delay between the occurrences of the day maximum EEJ and well-developed EIA. This indicates that the diurnal characteristics of the EEJ can provide the information about the EIA characteristics few hours in advance.

The present study demonstrates that the day-to-day variability of EIA and the characteristic features of the anomaly crest exhibit strong dependence with the EEJ diurnal characteristics. This study also reveals that the EEJ could provide information of the EIA characteristics few hours in advance. Hence, quantitative studies on the role of EEJ on EIA characteristic features over different regions during different solar activity conditions will be of immense use for the improved predictions of TEC over the equatorial and low-latitude sectors.

(southern hemisphere) sectors. The magnetometer measurements during the low solar activity year 2004 are used to derive the EEJ values. Simultaneous GPS-TEC measurements from two different chains of stations along the common meridian of 77°E in the Indian sector and 45°W in the Brazilian sector are used to study the EIA variabilities. It is observed that the diurnal variations of EEJ show equinoctial maximum in both sectors. Significant day-to-day variability is observed in the diurnal variations of EEJ over the Indian and Brazilian sectors. The diurnal variations of TEC have also shown significant seasonal dependence with equinoctial maximum and summer minimum in the Indian sector and winter minimum in the Brazilian sector. TEC variations at all locations exhibit significant day-to-day variability, which is found to be more prominent at and around the anomaly crest locations during the equinoctial months. Simultaneous observations of EEJ and TEC around the anomaly crest locations reveal similar seasonal and day-to-day variability in their values. Semiannual behavior with two peaks in March/April and September/October is simultaneously observed in the EEJ and TEC variations over the equator and anomaly crests locations in the two hemispheres.

Acknowledgments

One of the authors, K.V., wish to express his sincere thanks to the Fundação de Amparo a Pesquisa do Estado de Sao Paulo (FAPESP), Sao Paulo, Brazil, for providing financial support through the process 2012/08445-9 and 2013/17380-0. C.M. Denardini thanks CNPq/MCTI (grant 303121/2014-9), FAPESP (grant 2012/08445-9), and to the Brazilian Government (Program 2056, Budget Action N387, Budget Plan 08/2013-2017), which supported both the scientific and infrastructure projects that gave birth to the Embrace Magnetometer Network and to the Embrace/INPE Program. The authors wish to express their sincere thanks to IBGE (http://www.ibge.gov.br/home/geociencias/geodesia/rbmc/rbmc_est.php) for providing GPS-TEC data over Brazil, to the GSFC, NASA for providing the TEC data over Brasilia (BRAZ) (http://cdaweb.gsfc.nasa.gov/istp_public/), and the Indian Institute of Geomagnetism for providing magnetometer data in the Indian sector (<http://wdciq.res.in/WebUI/Home.aspx>). One of the authors, K.V., wishes to express his heartfelt gratitude to his mentor late P.V.S.Rama Rao for his invaluable suggestions.

References

- Abbas, M., B. D. B. Joshua, I. A. Adimula, A. B. Raibu, and O. R. Bello (2012), Variability of electrojet strength along the magnetic equator using MAGDAS/CPMN data, *J. Inf. Data Manage.*, *1*(1), 10–13. [Available at <http://researchpub.org/journal/jidm/number/vol1-no1-2.pdf>.]
- Abdu, M. A., I. S. Batista, and J. R. deSouza (1996), An overview of IRI-observational data comparison in American (Brazilian) sector low latitude ionosphere, *Adv. Space Res.*, *18*(6), 13–22, doi:10.1016/0273-1177(95)00893-4.
- Alex, S., and S. Mukherjee (2001), Local time dependence of the equatorial counter electrojet effect in a narrow longitudinal belt, *Earth Planets Space*, *53*, 1151–1161. [Available at <http://svr4.terrapub.co.jp/journals/EPS/pdf/2001/5312/53121151.pdf>.]
- Bagiya, M. S., H. P. Joshi, K. N. Iyer, M. Aggarwal, S. Ravindhran, and B. M. Pathan (2009), TEC variations during low solar activity period (2005–2007) near the equatorial ionospheric anomaly crest region in India, *Ann. Geophys.*, *27*, 1047–1057, doi:10.5194/angeo-27-1047-2009.
- Baker, W. G., and D. F. Martyn (1953), Electric current in the ionosphere, The conductivity, *Philos. Trans. R. Soc. London*, *246*(A913), 281–294, doi:10.1098/rsta.1953.0016.
- Brunini, C., M. A. Van Zele, A. Meza, and M. Gende (2003), Quiet and perturbed ionospheric representation according to the electron content from GPS signals, *J. Geophys. Res.*, *108*(A2), 1056, doi:10.1029/2002JA009346.
- Chandra, H., H. S. S. Sinha, and R. G. Rastogi (2000), Equatorial electrojet studies from rocket and ground measurements, *Earth Planet Space*, *52*(2), 111–120. [Available at <http://link.springer.com/article/10.1186%2FBF03351619>.]
- Chandrasekhar, N. P., K. Arora, and N. Nagarajan (2014), Characterization of seasonal and longitudinal variability of EEJ in the Indian region, *J. Geophys. Res. Space Physics*, *119*, 10,242–10,259, doi:10.1002/2014JA020183.
- Chapman, S. (1951), The equatorial electrojet as detected from the abnormal electric current distribution about Huancayo, Peru and elsewhere, *Arch. Meteorol. Geophys. Bioklimatol., Ser. A*, *4*(1), 368–390. [Available at <http://link.springer.com/article/10.1007%2FBF02246814>.]
- Chapman, S., and J. Bartels (1940), *Geomagnetism*, vol. 1 and 2, Oxford Univ. Press. (Clarendon), London and New York.
- Denardini, C. M., M. A. Abdu, H. C. Aveiro, L. C. A. Resende, P. D. S. C. Almeida, E. P. A. Olivio, J. H. A. Sobral, and C. M. Wrasse (2009), Counter electrojet features in the Brazilian sector: Simultaneous observation by radar, digital sounder and magnetometers, *Ann. Geophys.*, *27*, 1593–1603, doi:10.5194/angeo-27-1593-2009.
- Denardini, C. M., L. C. A. Resende, J. Moro, M. Rockenbach, P. R. Fagundes, M. A. Gende, S. S. Chen, N. J. Schuch, and A. Petry (2013), The South American K index: Initial steps from the embrace magnetometer network, *Proc. of the 13th International Congress of the Brazilian Geophysical Society & EXPOGEF, Rio de Janeiro, Brazil 26–29 August 2013*, 1901–1905, doi:10.1190/sbgf2013-391.
- Doumouya, V., and Y. Cohen (2004), Improving and testing the empirical equatorial electrojet model with CHAMP satellite data, *Ann. Geophys.*, *22*, 3323–3333, doi:10.5194/angeo-22-3323-2004.
- Doumouya, V., J. Vassal, Y. Cohen, O. Fambitakoye, and M. Menvielle (1998), Equatorial electrojet at African longitudes: First results from magnetic measurements, *Ann. Geophys.*, *16*, 658–666, doi:10.1007/s00585-998-0658-9.
- Doumouya, V., Y. Cohen, B. R. Arora, and K. Yumoto (2003), Local time and longitude dependence of the equatorial electrojet magnetic effects, *J. Atmos. Terr. Phys.*, *65*(14–15), 1265–1282, doi:10.1016/j.jastp.2003.08.014.
- Fambitakoye, O. (1976), Equatorial electrojet and regular daily variation SR-II. The centre of the equatorial electrojet, *J. Atmos. Terr. Phys.*, *38*(1), 19–26, doi:10.1016/0021-9169(76)90189-6.
- Fambitakoye, O., and P. N. Mayaud (1976), The squatorial electrojet and regular daily variation SR. I. A determination of the equatorial electrojet parameters, *J. Atmos. Terr. Phys.*, *38*, 1–17, doi:10.1016/0021-9169(76)90188-4.
- Forbes, J. M. (1981), The equatorial electrojet, *Rev. Geophys. Space Phys.*, *19*(3), 469–504, doi:10.1029/RG019i003p00469.
- Forbush, S. E., and M. Casaverde (1961), *The Equatorial Electrojet in Peru*, 620 pp., The Kirby Lithographic Company, Inc., Washington, D. C. [Available at <http://catalog.hathitrust.org/Record/001639508>.]
- Gouin, P., and P. N. Mayaud (1967), A propos de l'existence possible d'un "contre-electrojet" aux latitudes magnetiques equatoriales, *Ann. Geophys.*, *23*, 41–47.
- Guizzelli, L. M., C. M. Denardini, J. Moro, and L. C. A. Resende (2013), Climatological study of the daytime occurrence of the 3-meter EEJ plasma irregularities over Jicamarca close to the solar minimum (2007 and 2008), *Earth Planets Space*, *65*, 39–44, doi:10.5047/eps.2012.05.008.
- Jee, G., R. W. Schunk, and L. Scherliess (2005), On the sensitivity of total electron content (TEC) to upper atmospheric/ionospheric parameters, *J. Atmos. Sol. Terr. Phys.*, *67*(11), 1040–1052, doi:10.1016/j.jastp.2005.04.001.
- Kane, R. P. (1976), Geomagnetic field variations, *Space Sci. Rev.*, *18*, 413–540. [Available at <http://link.springer.com/article/10.1007/BF00217344>.]
- Kane, R. P., and N. B. Trivedi (1982), Comparison of equatorial electrojet characteristics at Huancayo and Eusebio (Fortaleza) in the South American region, *J. Atmos. Terr. Phys.*, *44*(9), 785–792, doi:10.1016/0021-9169(82)90007-1.
- Mannucci, A. J., B. D. Wilson, D. N. Yuan, C. M. Ho, U. J. Lindqwister, and T. F. Runge (1998), A global mapping technique for GPS derived ionospheric total electron content measurements, *Radio Sci.*, *33*, 565–582, doi:10.1029/97RS02707.
- Mayaud, P. N. (1977), The equatorial counter electrojet – A review of its geomagnetic aspects, *J. Atmos. Terr. Phys.*, *39*(9–10), 1055–1070, doi:10.1016/0021-9169(77)90014-9.
- Mazaudier, A. C., et al. (2006), Sun-Earth System Interaction studies over Vietnam: An international cooperative project, *Ann. Geophys.*, *24*, 3313–3327, doi:10.5194/angeo-24-3313-2006.
- Mazaudier, C., et al. (1993), International equatorial electrojet year, *Braz. J. Geophys.*, *11*(3), 303–317.
- Mazaudier, C. A., et al. (2005), On equatorial geophysics studies: A review on the IGRGEA results during the last decade, *J. Atmos. Terr. Phys.*, *67*, 301–313, doi:10.1016/j.jastp.2004.10.001.
- Muniz, B. L. (1992), The equatorial electrojet: A brief review, *Geofisica Internacional*, *31*(2), 115–120. [Available at <http://www.revistas.unam.mx/index.php/geofisica/article/view/39477>.]
- Onwumechili, C. A. (1967), Geomagnetic variations in the equatorial zone, in *Physics of Geomagnetic Phenomena*, vol. 1, Chap.III-2, edited by S. Matsushita and W. H. Campbell, pp. 425–507, Academic Press, New York.
- Rabiu, A. B., N. Nagarajan, F. N. Okeke, and E. A. Anyibi (2007), A study of day-to-day variability in geomagnetic field variations at the electrojet zone of Addis Ababa, East Africa, *Afr. J. Sci. Tech.*, *8*(2), 54–63.
- Rastogi, R. G. (1989), The equatorial electrojet: Magnetic and ionospheric effects, in *Geomagnetism*, vol. 3, chap. 7, pp. 461–525, edited by J. A. Jacobs, Academic Press, London.
- Rastogi, R. G., H. Chandra, S. Rahul, N. B. Trivedi, and S. L. Fontes (2013), A comparison of equatorial electrojet in Peru and east Brazil, *Open Atmos. Sci. J.*, *7*, 29–36, doi:10.2174/1874282320130417003.
- Reddy, C. A. (1981), The equatorial electrojet: A review of the ionospheric and geomagnetic aspects, *J. Atmos. Terr. Phys.*, *43*(5–6), 557–571, doi:10.1016/0021-9169(81)90118-5.
- Reddy, C. A. (1989), The equatorial electrojet, *Pure Appl. Geophys.*, *131*(3), 485–508. [Available <http://link.springer.com/article/10.1007%2FBF00876841>.]

- Richmond, A. D. (1973), Equatorial electrojet—I. Development of a model including winds and electric field, *J. Atmos. Terr. Phys.*, *35*(6), 1083–1103, doi:10.1016/0021-9169(73)90007-X.
- Shimeis, A., C. A. Mazaudier, R. Fleury, A. M. Mahrous, and A. F. Hassan (2014), Transient variations of vertical total electron content over some African stations from 2002 to 2012, *Adv. Space Res.*, *54*, 2159–2171, doi:10.1016/j.asr.2014.07.038.
- Shimeis, A., C. Borries, C. A. Mazaudier, R. Fleury, A. M. Mahrous, A. F. Hassan, and S. Nawar (2015), TEC variations along an East Euro-African chain during 5th April 2010 geomagnetic storm, *Adv. Space Res.*, *55*, 2239–2247, doi:10.1016/j.asr.2015.01.005.
- Stening, R. J. (1985), Modeling the equatorial electrojet, *J. Geophys. Res.*, *90*(A2), 1705–1719, doi:10.1029/JA090iA02p01705.
- Sugiura, M., and J. C. Cain (1966), A model equatorial electrojet, *J. Geophys. Res.*, *71*(7), 1869–1877, doi:10.1029/JZ071i007p01869.
- Sugiura, M., and D. J. Poros (1969), An improved model equatorial electrojet with a meridional current system, *J. Geophys. Res.*, *74*(16), 4025–4034, doi:10.1029/JA074i016p04025.
- Venkatesh, K., P. R. Fagundes, G. K. Seemala, R. de Jesus, A. J. de Abreu, and V. G. Pillat (2014), On the performance of the IRI-2012 and NeQuick2 models during the increasing phase of the unusual 24th solar cycle in the Brazilian equatorial and low-latitude sectors, *J. Geophys. Res. Space Physics*, *119*, 5087–5105, doi:10.1002/2014JA019960.
- Yamazaki, Y., A. D. Richmond, A. Maute, H.-L. Liu, N. Pedatella, and F. Sassi (2014), On the day-to-day variation of the equatorial electrojet during quiet periods, *J. Geophys. Res. Space Physics*, *119*, 6966–6980, doi:10.1002/2014JA020243.